

Mechanisms of Phase Transformation and Creating Mechanical Strength in a Sustainable Calcium Carbonate Cement

Jesús Rodríguez-Sánchez^{1,2}, Teresa Liberto^{3,4}, Catherine Barentin^{3,5} and Dag Kristian Dysthe¹.

¹Physics of Geological Processes (PGP), The NJORD Centre, Department of Physics, University of Oslo, PO Box 1048 Blindern, Oslo, Norway.

²The Department of Materials Science and Engineering, The University of Sheffield, Sheffield, S10 2TN, UK

Institute of Materials Science and Technology, TU Wien, Getreidemarkt 9, 1060
³Wien, Austria

⁴Institut Lumière Matière, F-69622, Université Claude Bernard Lyon 1, CNRS, Villeurbanne, France.

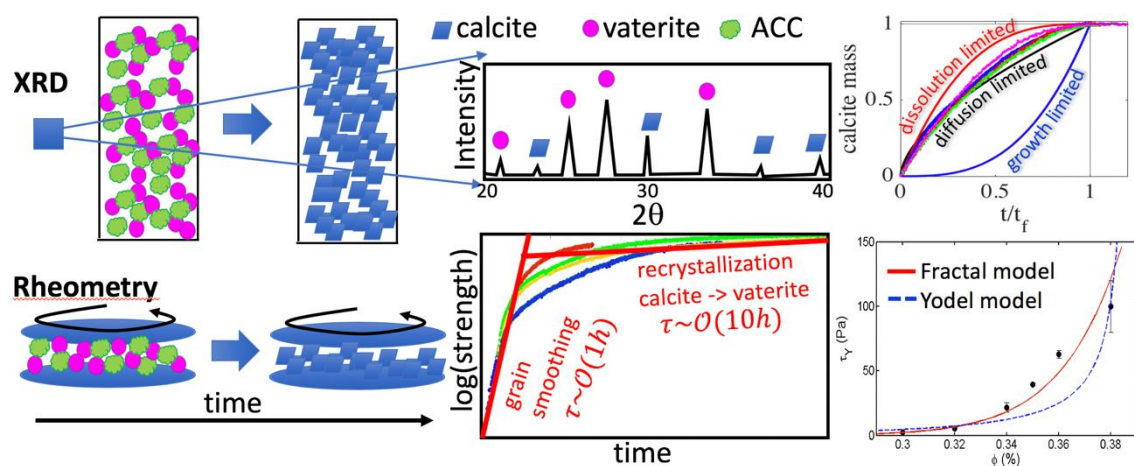
⁵Institut Universitaire de France, France.

Abstract

Calcium carbonate cements have been synthesized by mixing amorphous calcium carbonate and vaterite powders with water to form a cement paste and study how mechanical strength is created during the setting reaction. In-situ XRD was used to monitor the transformation of ACC and vaterite phases into calcite and a rotational rheometer was used to monitor the strength evolution. There are two characteristic time scales of the strengthening of the cement paste. The short timescale of the order 1 hour is controlled by smoothening of the vaterite grains, allowing closer and therefore adhesive

contacts between the grains. The long timescale of the order 10-50 hours is controlled by the phase transformation of vaterite into calcite. This transformation is, unlike in previous studies using stirred reactors, found to be mainly controlled by diffusion in the liquid phase. The evolution of shear strength with solid volume fraction is best explained by a fractal model of the paste structure.

Keywords: calcium carbonate cement; setting reaction; (re)crystallization kinetics; cement strengthening; crystal bridging



Graphical abstract

1. Introduction

Due to the carbon footprint of ordinary Portland cement (OPC) there has been an increased interest in alternative hydraulic binders [1–4]. Inspired by the outstanding mechanical properties of limestone, which is mainly composed of calcium carbonate (CaCO_3), alternative production paths to form calcium carbonate binders have been

investigated [1,5,6], the most famous being the Calera carbonation process [7]. Another path to prepare pure CaCO_3 cements is of special interest as a model system: Combes and co-workers [5,6] mixed water with two metastable CaCO_3 phases. One of them is the highly reactive amorphous calcium carbonate, ACC, while the other is one of the metastable crystalline phases, either vaterite, V, or aragonite, Ar. The polymorphs ACC and V or A recrystallize into the most stable polymorph, calcite, during the setting of the cement.

However, the mechanical properties still remain poorly understood despite their chemical similarities with limestone. These properties develop during the process of preparing the initial powders, mixing the paste, setting reactions at constant liquid fraction and during drying. In this paper, we focus on the properties of a calcium carbonate paste while it is transforming from ACC and vaterite to calcite, at constant liquid fraction. We combine measurements of the phase transformation with rheological properties and interpret this in terms of mechanisms of chemical, physical and structural changes. This double approach allows us to link the microscopic properties with the mechanical properties of the paste.

Recrystallization of CaCO_3 polymorphs has received much attention the later years [8–16] due to the importance of CaCO_3 in industry [17], climate [18], biomineralization [19] and geology [20]. This large body of knowledge on recrystallization mechanisms has yet to be put into the context of CaCO_3 cement setting. In this paper, we compare CaCO_3 setting reactions with the transformation mechanisms in other settings and then we compare this to the development of elastic properties of the CaCO_3 cement paste during setting.

Rheological measurements are efficient tools to investigate the structure of concentrated pastes and the interaction between particles [21]. In particular, the range of solid fractions for which elastic or yield stress behaviour appear allows to determine the sign of the interparticle forces. In the case of attractive colloidal gels, the pastes are composed by a continuous percolating network of aggregated particles characterised by a fractal dimension. Models of mechanical deformation of such networks link the structure, the solid fraction and the elastic modulus or yield stress [22–24].

Most studies of rheology of concentrated particle suspensions (pastes) have been performed on timescales where the particles do not react although some studies of setting cement pastes have been performed [25]. In the present system, however, the initial particles (ACC and vaterite) of the paste disappear completely while new calcite particles are forming. The properties of hardened CaCO_3 cements are a result of the (re)crystallization that the paste undergoes when the solid reagents are mixed with water. It is therefore of crucial importance to correlate these phase transformations with the evolution of the viscoelastic properties of the paste during maturation to unravel the strengthening mechanisms and their kinetics [26,27].

In the present study, sustainable pure calcium carbonate cements have been synthesized following “Combes’ method” [6]. *In-situ* X-ray diffraction (XRD) scans and rheological measurements have been carried out to investigate the interplay between i) the transformation kinetics of each phase (ACC, vaterite and calcite) of the paste and ii) the development of mechanical properties during setting.

2. Materials and methods

CaCO₃ cement samples with diverse mixture design have been prepared. Both the composition and the (re)crystallization kinetics of each CaCO₃ phase (ACC, vaterite and calcite) along setting and hardening processes have been studied by in-situ time-lapse X-ray diffraction (XRD). Then, the effect of ACC and vaterite (re)crystallization on the viscoelastic properties of the pastes have been quantified by rheological measurements.

2.1. Synthesis of CaCO₃ polymorphs

The preparation of CaCO₃ cements requires the synthesis of different calcium carbonate polymorphs in order to design the initial cement mixture [6]. Accordingly, both ACC and vaterite phases were precipitated by mixing calcium chloride (CaCl₂·6H₂O, Sigma Aldrich) and sodium carbonate (Na₂CO₃, Sigma Aldrich) equimolar (0.5 M) solutions, prepared with ultrapure Milli-Q water (18.2 MΩ cm), at room temperature using a magnetic stirrer set at 400 rpm. Following Ogino et al. [8] we used reaction time 10 sec for ACC and 30 min for vaterite. To wash off any dissolved sodium chloride (NaCl), the CaCO₃ precipitates were rinsed with deionized water and ethanol, using a filtering kit and 0.5 μm pore-size filter papers (Millipore, USA). Subsequently, the CaCO₃ precipitates were flushed with liquid N₂ to stop the recrystallization of these metastable phases. The frozen precipitates were lyophilized (Alpha 1-4 LD plus, Martin Christ, Germany) for 48 h at 0.05 mbars and -50 °C and stored in a freezer (-22°C) with additional silica powder bags to keep them as dry as possible [13] prior to cement manufacturing.

The precipitates were scanned by X-ray diffraction (XRD) (Bruker D8 Discover X-ray diffractometer) to identify the crystalline phases present using Cu Kα radiation (30 mA and 40 kV) and recording 2θ angles from 20 to 50° at a 0.04 s⁻¹ sweep rate. Additionally,

they were imaged with scanning electron microscopy (SEM) (Hitachi SU5000 Field-Emission; 1kV acceleration voltage and 3.0 mm working distance).

2.2. In-situ XRD analysis during setting and hardening

To quantify the composition and the (re)crystallization kinetics of CaCO_3 cement pastes during the setting and hardening processes, we have used *in-situ* time-lapse X-ray diffraction (XRD) (Bruker D8 A25 X-ray diffractometer). Five CaCO_3 cement pastes were made up of mixtures of ACC and vaterite powders in different weight ratios (wt.%): 1:0, 1:1, 1:2, 1:3 and 0:1 wt.%, with a solid volume concentration, Φ , equal to 46%. This concentration was deduced from the total powder weight and ACC, vaterite and water densities. Just after mixing the powders with the liquid phase, the resulting pastes were viscous and easily mouldable for several minutes and they were moulded into the sample holder (disk of 25 mm diameter, 2 mm depth), firmly tamped and covered with a plastic film immediately after mixing with water to avoid drying.

XRD patterns were recorded every 5 min for a maximum of 60 hours using Mo $K\alpha$ radiation (48 mA and 48 kV) and recording 2θ angles from 10° to 17° at a sweep rate of 0.035 s^{-1} . Since the mass of a crystalline phase, m_i , is proportional to the area, A_i , under its diffraction peak, the net area under the main vaterite and calcite diffraction peaks (located at 12.35° and 13.39° , respectively within the range scanned) were calculated using the software Diffrac.Suite EVA (Bruker AXS, USA) for each scan. The mass fractions of each phase, X_i , can be calculated from A_i based on two assumptions: the initial vaterite mass fraction is the same as prepared in the mixture proportions and in the final scan the cement is pure calcite minus the unreacted vaterite. Then the mass fractions of calcite, vaterite and ACC can be calculated by $X_V(t) = X_V(t_0) \cdot \frac{A_V(t)}{A_V(t_0)}$, $X_C(t) =$

$\frac{A_C(t)}{A_C(t_f)}(1 - X_v(t_f))$ and $X_{ACC} = 1 - X_C - X_V$, where t represents the time, t_0 the initial time, t_f the final time and $X_V(t_0)$ the starting vaterite mass fraction which is determined by the mixture design, i.e., either 0, 0.5, 0.66, 0.75 or 1, for the ACC:V 1:0, 1:1, 1:2, 1:3 and 0:1 wt.% pastes, respectively.

2.3. Rheological characterization

2.3.1. Sample preparation

CaCO₃-cement colloidal suspensions were prepared by dispersion of ACC and vaterite powdered mixtures in distilled water. Three different mixtures were made up by mixing ACC and vaterite powders in different weight ratios (wt.%): 1:1, 1:2 and 1:3, respectively. The selected solid volume concentration, Φ , was 36% based on preliminary tests to determine the suitable concentration range for rheological measurements (storage modulus, $G' > \text{loss modulus}, G''$). We could not study higher concentrations, Φ , due to some limitations of the rheometer and in particular due to its maximal torque. This concentration was deduced from the total powder weight and ACC and vaterite densities within the paste. The mixing of the solid and the liquid phase was carried out in a vortex stirrer (Ultra Turrax TD300) at 5800 rpm for 20 seconds. This time was checked to be long enough to assure a homogeneous and easily mouldable paste without modifying its viscoelastic properties. After the mixing step, the samples were immediately transferred into the rheometer geometry and studied.

2.3.2. Measurement protocols

The viscoelastic properties of the cement pastes (ACC:V mixtures) were studied using a stress-controlled rotational rheometer (Anton Paar MCR 301) in oscillating mode. The

measurements were carried out using a plate-plate geometry (36 and 64 mm, upper and lower diameters, respectively) at room temperature. The gap between the two plates was fixed to 1 or 2 mm. Both plates were covered with sand-paper PV 320 (roughness 46 μm) to prevent slippage [28]. This was checked using diffusing-wave spectroscopy (DWS) across the rheometer gap [29]. In addition, a moisture chamber was used to assure a water-saturated atmosphere and thus dispel any paste drying effect during the data acquisition.

From the measurements, the storage modulus, G' , and the loss modulus, G'' , were extracted as the characterizing parameters of the viscoelastic behaviour. Those are defined by [21]:

$$G^* = G' + iG'' \quad (1)$$

where G^* is the complex modulus, being the ratio between the complex stress, σ^* , and the complex strain, γ^* :

$$\sigma^*(t) = G^* \cdot \gamma^*(t) \quad (2)$$

Two different experimental protocols were used. The first one aimed at studying the evolution of the ACC and vaterite transformation reaction by measuring the time evolution of the storage modulus $G'(t)$ during 10 hours. The second one aimed at characterizing the elastic properties of the CaCO_3 cement paste just after its preparation.

2.3.2.1. Viscoelastic measurements during setting reaction: aging experiment

To quantify the influence of ACC and vaterite recrystallization into calcite on the macroscopic mechanical properties of pastes, a constant oscillatory deformation, $\gamma = 0.003\%$, was applied to the pastes at the imposed frequency $f = 10$ Hz, for several hours.

This experiment allows measuring the time evolution of the viscoelastic moduli (G' , G'') during the setting reaction in the linear regime. Indeed the values of strain and frequency ($\gamma = 0.003\%$, $f=10$ Hz) were chosen small enough to ensure measurements within the linear elastic regime for all the tested pastes, and thus no perturbation of the setting and hardening dynamics of the samples. The measurements started immediately after mixing the solid and the liquid phase, transferring the pastes into the plate-plate geometry and sealing the setup with the moisture chamber.

2.3.2.2 Viscoelastic properties and yield stress of initial pastes

The pastes were prepared as described on Section 2.3.1., and transferred into the plate-plate setup sealed with the moisture chamber. In the aim to characterize the viscoelasticity and the yield stress of fresh paste, increasing stresses are imposed and resulting strains are measured. At low stresses and low strains, the storage modulus, G' , is constant so the linear storage modulus, G'_{lin} , can be estimated precisely. At larger strains, the pastes eventually yield and become liquid-like, causing the storage modulus, G' , to break down. The end of the linear regime, i.e., the onset of plasticity, was characterized by the critical strain, γ_{CR} , which corresponds to the value of γ for which the storage modulus was 10-15% lower than the value in the elastic regime, G'_{lin} [28].

3. Results and discussion

We present the XRD measurements corresponding to the recrystallization of calcium carbonate polymorphs from amorphous calcium carbonate (ACC) and vaterite (V) to the final calcite cement. Subsequently, the time evolution of the paste rheology is presented.

Two different timescales of transformation by recrystallization, particle interactions and strength development are identified and modelled.

3.1. Characterization of CaCO_3 precipitates

To check the validity of the synthesis protocols described for both ACC and vaterite, the dried precipitates used as starting materials for the different cement compositions are investigated by SEM and XRD. The SEM analysis indicates that ACC precipitates (Figure 1A) consist of equidimensional spherical nanoparticles (<50 nm in diameter) accompanied by rhombohedral crystals of about 50-100 nm. These are interpreted to be calcite and confirmed by XRD analysis (Figure 1D). Vaterite precipitates (Figure 1B) consist of spherical grains of 4-5 μm in diameter also accompanied by rhombohedral grains (4-5 μm), which are calcite (Figure 1C) according to the XRD scans (Figure 1D). An analysis of the XRD patterns using the software Diffrac. Suite TOPAS (Bruker AXS, USA) derived a composition of 86% ACC and 14% calcite for ACC precipitates while a 93% vaterite and 7% calcite for vaterite precipitates.

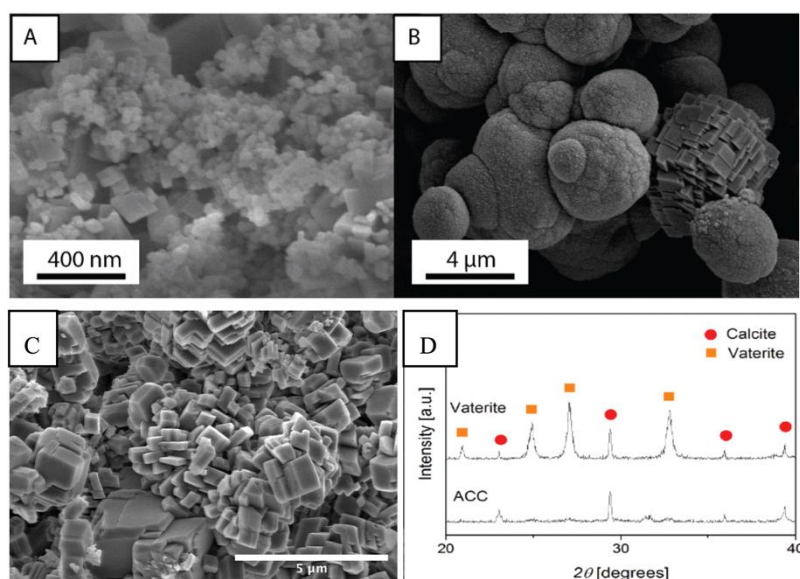


Figure 1. SEM micrographs of synthesized calcium carbonate powders in the form of (A) ACC phase and (B) vaterite phase with one calcite grain. (C) Calcite cement after recrystallization of ACC:V 1:3 mixture. Typical grain size varies from 0.3 to 1 μm with a few larger and smaller. The calcite grains are faceted, and grain boundaries seem to have been well developed. (D) XRD patterns of lyophilized ACC and vaterite powders. Some calcite will always be present in the initial powders.

3.2. Phase transformation during setting and hardening

3.2.1 Measurement of time evolution of different phases

The time evolution of the cement compositions during the setting reaction has been followed by *in-situ* time-resolved XRD. Figure 2 displays the calculated molar fractions, X_i , of the three calcium carbonate polymorphs (ACC, vaterite and calcite) that coexist during the process for three different CaCO_3 cement compositions (1:1, 1:2 and 1:3 wt.% ACC:V) as well as for pure ACC (ACC:V 1:0) and pure vaterite (ACC:V 0:1) pastes as references. It shows visually how the two starting phases – ACC and vaterite – are dissolving while the third one – calcite – is growing at the expense of the other two. One also observes that the rate of transformation slows down with time.

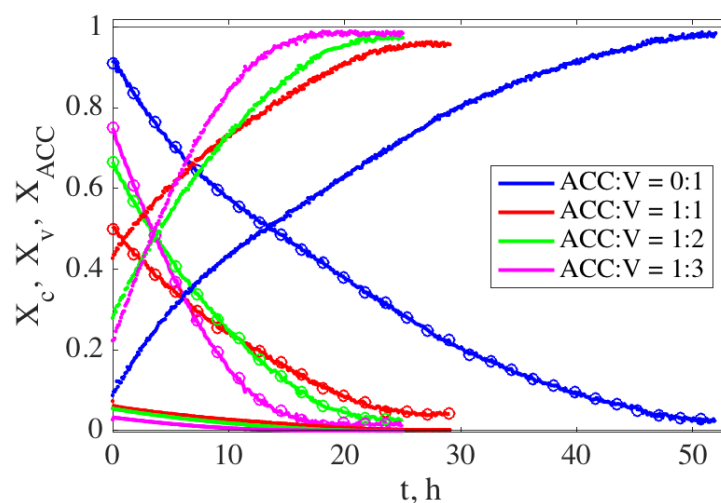


Figure 2. Calcite (increasing with time), vaterite (circles) and ACC (always below 0.1) mass fraction evolution with time for four different CaCO_3 cement compositions (0:1, 1:1, 1:2 and 1:3 wt.% ACC:V).

For the three cement compositions including both ACC and vaterite, the results show a clear trend: higher initial vaterite concentration leads to faster growth rates and faster recrystallization process. However, pure vaterite (ACC:V 0:1 wt.%) shows the slowest transformation kinetics, probably due to its lower free-energy difference, ΔG , (6.2 kJ.mol^{-1} [30]) with respect to calcite in comparison with ACC (15.0 kJ.mol^{-1} [14]). The ACC dissolves very quickly in all cases.

3.2.2 Analysis of phase transformation kinetics: rate-limiting step

The transformation of ACC through vaterite to calcite is dominated by the sequential process of 1) dissolution of vaterite, 2) diffusion of CaCO_3 from the dissolution site to a growth site and then 3) growth of calcite. If one of these three processes is significantly slower than the other ones, it is called the 'rate-limiting step'.¹ The dissolution (growth) *flux* at a solid-liquid interface is proportional to the thermodynamic driving force times a rate constant. The overall rate of dissolution (growth) in the system is therefore proportional to the surface area of the dissolving (growing) crystals. Since the vaterite surface area is initially large and diminishes, vaterite dissolution rate control predicts that the transformations will start out at a high rate and slow down. Since calcite surface area is initially small and growing, calcite growth rate control predicts that the transformations

¹ The aim of this paper is not to study the intricate details of ACC to calcite transformation. This has been done in stirred reactors in a large number of studies. The aim here is to elucidate the effective behaviour in a porous system: a setting cement.

will start out at a low rate and accelerate. Since surface area of the crystals scales with the mass to the power 2/3 we may write

$$\frac{dm_c}{dt} \propto m_c^{2/3} \Rightarrow X_c \propto \left(\frac{t}{t_f}\right)^3 \quad (3)$$

for calcite growth control and

$$\frac{dm_v}{dt} \propto -m_v^{2/3} \Rightarrow X_v \propto \left(1 - \frac{t}{t_f}\right)^3 \Rightarrow X_c \propto 1 - \left(1 - \frac{t}{t_f}\right)^3 \quad (4)$$

for vaterite dissolution control. The final time t_f is the time when the mass fraction reaches the final plateau value.

If diffusion from dissolution site to growth site is rate limiting, one has to make some assumption about what the diffusion distance is. Assuming that the size of the calcite grains is the pertinent length scale, the diffusion limited model of the calcite mass fraction can be expressed as (see Supplementary Material):

$$X_c \propto \left(\frac{t}{t_f}\right)^{3/5}. \quad (5)$$

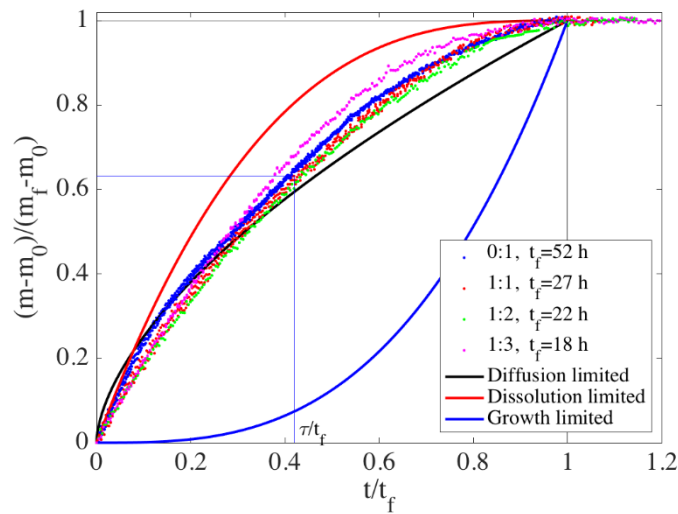


Figure 3. Mass evolution with normalized time for four different CaCO_3 cement compositions (0:1, 1:1, 1:2 and 1:3 wt.% ACC:V). The solid line shows the predicted evolution from models with diffusion, vaterite dissolution and calcite growth as the rate-limiting steps.

In Figure 3 we have rescaled the time evolution of the vaterite and calcite mass by the initial and final mass and rescaled the time by the final time, t_f . This rescaling collapses all the data onto a single curve that can be compared to the three models of rate-limiting step: diffusion, dissolution and growth (see Supplementary Material for more details). It is immediately clear that the transformations ACC - vaterite - calcite in a cement paste is not limited by the calcite growth. In previous studies, using stirred liquid reactors where 1 M solutions of CaCl_2 and Na_2CO_3 are mixed, the overall transformation from ACC to calcite was calcite growth rate controlled [8,11] (like the blue line in Figure 3). There are two main reasons why our result is so radically different: 1) cements and porous media are not stirred and 2) heterogeneous nucleation of calcite in a cement lowers the nucleation barrier and increases the surface area for growth. In a stirred liquid reactor the main point is to avoid diffusion limitation of the rates so that pure reaction rates may be measured. However, nucleation seems to be a limit to the general validity of the stirred

liquid reactor results since independent measurements of the dissolution and growth rates of vaterite and calcite find that calcite rate constant is 2-10 times larger than the vaterite dissolution constant [31–33]. In a cement or porous media on the other hand there will be some influence of diffusion unless the growing phase is nucleated everywhere. The data presented in Figure 3 falls somewhere between the simple diffusion limited model - with calcite radius as the diffusion length scale - and the dissolution limited model.

To compare the time scale of phase transformations with the time scales of rheology, we use a standard definition of the relaxation time τ : $\ln[(m_0 - m)/(m_f - m_0)] = \ln[X] = t/\tau$, that is $\tau \sim 0.4 t_f$. The relaxation times are then $\tau_{\text{ACC:V } 1:1} = 11 \text{ h}$, $\tau_{\text{ACC:V } 1:2} = 9 \text{ h}$, $\tau_{\text{ACC:V } 1:3} = 7 \text{ h}$ and $\tau_{\text{ACC:V } 0:1} = 20 \text{ h}$.

3.3. Viscoelasticity of CaCO_3 pastes

Here we study the time evolution of the elastic properties during the setting of the pastes. This evidences the existence of two distinct timescales: a short one of the order of the hour and a longer one that is consistent with the characteristic time of the phase transition. Finally we interpret the rheological measurements using colloidal gel model in the aim to provide insights on the paste microstructure and on the interaction between calcite grains.

3.3.1. Measurement of time evolution of viscoelastic properties

In order to map the strength evolution of the paste during recrystallization, we measured the viscoelastic properties with time. The storage modulus, G' , is typically one order of magnitude larger than the loss modulus, G'' (not shown), revealing the elastic-like behaviour of the pastes. Figure 4 presents the evolution of the storage modulus, G' , over

5-6 hours for three different CaCO_3 cement pastes. For each composition, we show the fastest and the slowest recorded evolutions.

One observes that the initial rigidity of the pastes depends on the composition and that its value increases as the ACC:V ratio decrease. Because vaterite particles are one order of magnitude smaller than ACC particles (see Figure 1), a smaller ACC:V ratio corresponds to larger number of particles and smaller interparticle distances. Since the interparticle forces are short range, the rigidity of the paste should increase as the ACC:V ratio decreases. This dependence has been reported previously not only for cement pastes but for several systems [34,35].

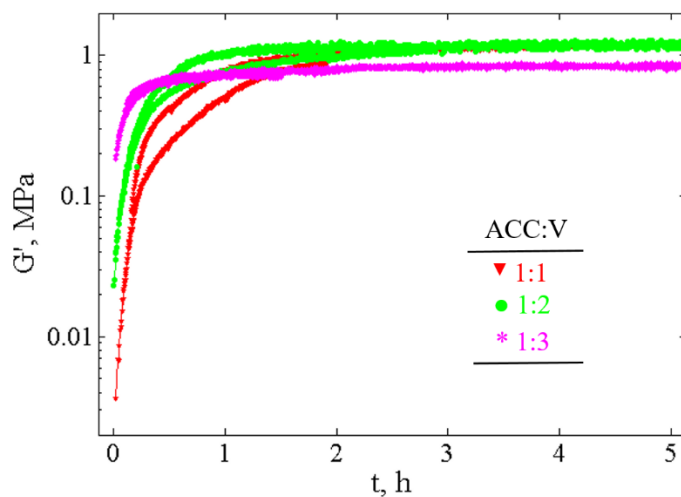


Figure 4. Time evolution of storage modulus, G' , for three different CaCO_3 cement compositions (ACC:V 1:1, 1:2 and 1:3 wt.%) measured at constant frequency, $f=10$ Hz, and deformation, $\gamma=0.003\%$.

For all studied pastes, the storage modulus, G' , increases progressively with time until it reaches a value of ~ 1 MPa independent of the composition. It is remarkable that even though all the original solid material is dissolved in the paste, the storage modulus never

decreases. Further insights from the data can be extracted by plotting the normalized final storage modulus G'_N defined as:

$$G'_N = \frac{G'(t_f) - G'(t)}{G'(t_f) - G'(t_0)} \quad (6)$$

where t_0 is the initial time and t_f is the final time (~6-10 hours) as the plateau value is reached. This definition allows studying the time dependence of the storage modulus independently of its initial value and indicates the distance to the final value. Due to the subtraction ($G'(t_f) - G'(t)$), a decrease of G'_N corresponds to an increase of G' . Figure 5 shows the time evolution of G'_N , for the three different CaCO_3 cement pastes examined here. One observes two distinct time scales; first a short time scale τ'_1 (steep slope) then a long time scale τ'_2 (small slope), that are determined by $\ln G'_N = -t/\tau'_i$. The calculated characteristic times averaged over all the measurements, τ'_1 , are 0.8 ± 0.1 h, 0.4 ± 0.02 h and 0.2 ± 0.02 h, and τ'_2 , are 4 ± 1 h, 5 ± 1 h and 6 ± 1 h for ACC:V 1:1, 1:2 and 1:3 compositions, respectively. The long time scale is of the same order of magnitude as the characteristic time of phase transformation.

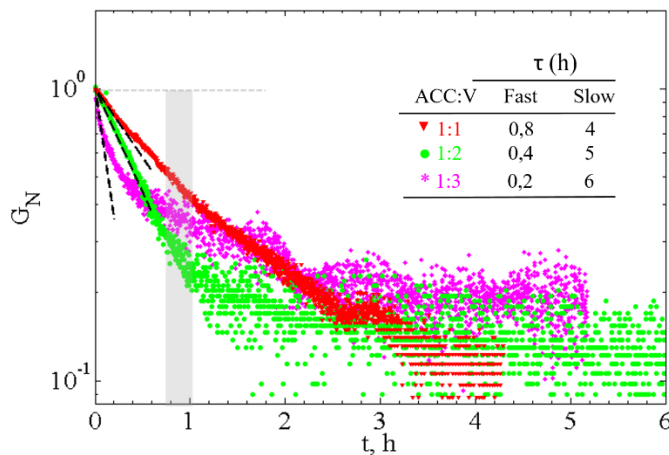


Figure 5. Time evolution of the normalized storage modulus, G_N' , for three different CaCO_3 cement compositions (1:1, 1:2 and 1:3 wt.% ACC:V) measured from the time evolution of the elastic modulus. The average characteristic reaction times, τ_i , are also included.

The rheological measurements evidence a fast increase of G' with a timescale of typically 1/2 hour followed by a slow increase of G' with a timescale ~ 5 h. Then G' reaches a plateau of ~ 1 MPa, whose value is similar to G' measured for calcite pastes with faceted grains of 70 nm size [28].

3.3.2 Fast increase of elastic modulus: smoothing of grains

The first fast strengthening of the paste is too slow to be due to merely reorganization of the grain packing. The rotational diffusion coefficient suggests reorganization on characteristic time of less than a second. We will argue that smoothing of surfaces at grain contacts is the most likely controlling process. Indeed the roughness of the contact is crucial for the interaction between particles and consequently for the macroscopic mechanical properties.

Recent molecular dynamics simulations of calcite - calcite interactions in water [36] show that there is an attractive energy minimum of -50 mJ.m^{-2} at a distance of 0.8 nm (4 layers of water) between perfectly smooth surfaces and an attractive well width of less than 0.2 nm. If the surfaces are not flat, one needs to convolute the interaction potential with the roughness [37] which results in no attractive interactions between calcite particles for roughness larger than 3 nm, a result that agrees well with other simulations and experiments on calcite [38,39]. As a result, we expect that smoothing of a contact induces

an increase of the attraction between grains and consequently an increase of the storage modulus. We can also calculate the characteristic time of the smoothing process.

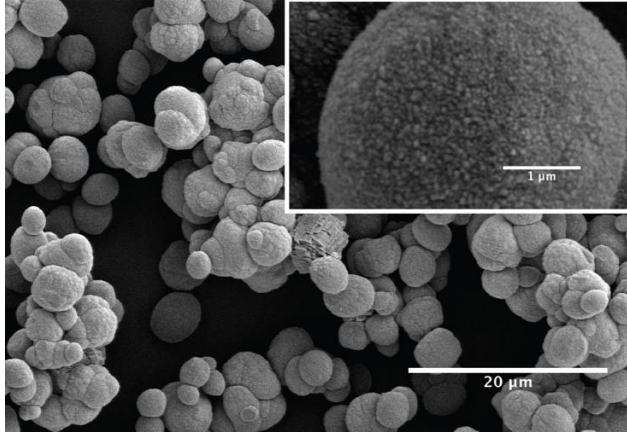


Figure 6: *Vaterite at initial stage of phase transformation. Inset: Magnification of a vaterite grain demonstrating the surface roughness consisting of ~100 nm spheres on the 2-5 μm large vaterite grains.*

As the ACC quickly dissolves, the paste is dominated by vaterite grains of characteristic radius $r_v = 2-5 \mu\text{m}$ with surfaces consisting of 100 nm spheroids (see Figures 1 and 6). The RMS roughness of the vaterite surface is initially of the order of 10 nm, causing initially a purely repulsive interaction between the vaterite grains. The radius of curvature of the small vaterite spheres ($r_s = 50 \text{ nm}$) causes an increase in the surface energy of the surface of $\Delta G = \gamma V_m (1/r_s - 1/r_v) = 150 \text{ J}\cdot\text{mol}^{-1}$ where, for the lack of vaterite surface energy, we have used the calcite surface energy. This chemical potential difference will drive local reordering and smoothing of the surface by recrystallization. Dissolution of the highest points will occur at a velocity of $v = V_m k_{d,v} \left(e^{\frac{\Delta G}{RT}} - 1 \right)^{0.86}$ [31]. Using $k_{d,v}$ of Cubillas et al [31], $v \sim 30 \text{ nm/h}$. If we assume that the dissolution of ~10 nm of the protruding spheres is the rate-limiting step it takes ~ 0.3 h to smooth the rough vaterite surfaces and achieving attractive interactions between the vaterite particles. This is the

same order of magnitude as the fast time scale of the increase of the storage modulus, 0.2-0.8 h. This suggests that the fast increase of the elastic modulus is due to an increase of the interacting area and consequently an increase of the attraction between grains.

3.3.3 Structure of the pastes

To go one step further and study the link between macroscopic properties (rheology) and microscopic properties (structure and interaction between grains), we explore in this section the structure of the initial paste (ACC:V). To do so, we study the influence of the volume fraction, denoted ϕ , on the elastic modulus G' and the yield stress τ_Y . These rheological properties are obtained by applying an amplitude sweep, i.e., an increasing oscillating deformation, to the pastes for all studied mixing ratios (1:1; 1:2, 1:3 wt.% ACC:V) and volume fractions. An example of such amplitude sweep is shown in Figure 7: the elastic modulus and the shear stress are plotted as a function of the shear strain. The elastic modulus exhibits first a plateau at small strains corresponding to the elastic linear regime, followed by a drastic decrease corresponding to the plastic and flow regimes. On the other hand, the shear stress increases first linearly with strain in the elastic regime then saturates as the paste enters in the plastic regime. Here the yield stress τ_Y is defined as the value of the shear stress at the beginning of the stress plateau reached for shear strain $\gamma \sim 5 \cdot 10^{-2} - 10^{-1} \%$.

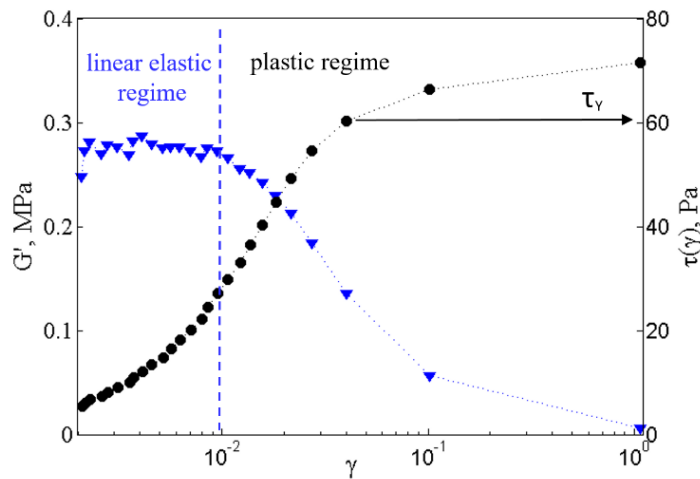


Figure 7: rheological properties of 1:2 ACC:V suspension of 36% volume fraction. The shear modulus G' (blue triangle down) and the shear stress τ (black circle) are plotted as a function of the shear strain γ measured through an amplitude sweep at $f=1\text{Hz}$. The vertical dashed line delineates the elastic and the plastic regimes. The horizontal plain line indicates the value of the yield stress defined as the value of the shear stress.

Note that these measurements are performed just after preparation of the paste, i.e. typically 10-15 minutes after mixing, and last for ~ 10 minutes. A drawback of this protocol is that the paste properties change during the measurement, but it allows us to estimate the volume-fraction range for which the initial suspension is a paste. More precisely, we manage to measure an elastic modulus and a yield stress for $20\% \leq \phi \leq 38\%$. This volume fraction range suggests [40] that flocculation occurs between grains. Indeed the volume fraction for which the yield stress diverges ϕ_{div} is much smaller than the maximum packing fraction of identical hard spheres (64%). Each floc is composed by aggregated particles and water, which explains the smaller value of the maximal volume fraction. To go one step further, we analyse the volume-fraction dependence of the yield stress $\tau_Y(\phi)$, in terms of Yodel's model [22] and of Shi's model [23,24] both developed for suspension of flocculated colloids (see Figure 8).

In short, Yodel's model consists in counting the interparticle bonds that cannot be broken and that are responsible for the yield stress. It takes into account the interparticle forces such as van de Waals or DLVO (Derjaguin-Landau-Verwey-Overbeek), the particle size, the maximum packing and the percolation threshold. For high volume fraction ($\phi > 25\%$), the percolation threshold can be neglected and the expected dependence of the yield stress with the volume fraction is expected to be:

$$\tau_Y \cong m \frac{\phi^3}{\phi_{div}(\phi_{div} - \phi)} \quad (7)$$

where m depends on the particle size and on the interaction between particles. The comparison between the Yodel model and our experimental data (see Figure 8) for ACC:V (1:2) paste suggests a maximum packing of 39%. However, the adjustment of the experimental data by this model is not very good, in particular the divergence of the yield stress with the volume fraction is not well taken into account.

We now turn to the Shi's model [23,24], a scaling theory that considers the colloidal gels as a dense suspension of flocs which are fractal objects composed by flocculated colloids. In this model, the rheological properties are set by the weakest link between particles or flocs. At high volume fractions, corresponding to our study, the weakest link is between flocs (named weak-link regime) and the yield stress is expected to depend on the volume fraction as a power law:

$$\tau_Y \sim m\phi^p \quad (8)$$

where m depends on the interparticle forces and the particle size and the exponent p depends on the fractal dimension d_f of the flocs. More precisely, $p = \frac{d+x}{d-d_f}$, where d is the Euclidean dimension and x the backbone of the clusters, often taken equal to 1 [28].

The adjustment of our data with the power law is quite satisfactory and suggests a fractal dimension of the flocs: $d_f \sim 2.76$.

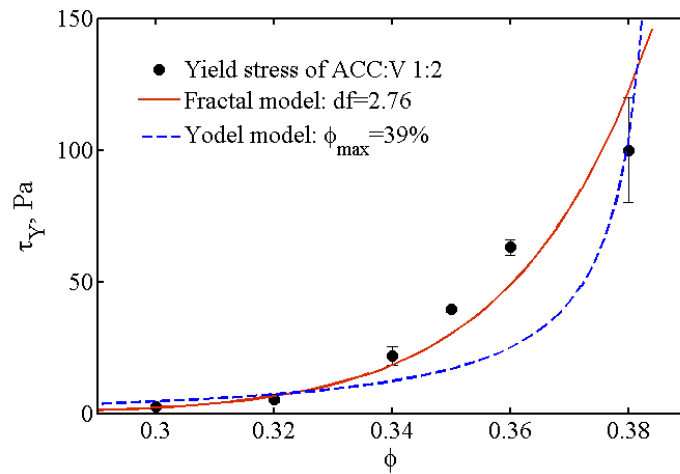


Figure 8: Dependence of the yield stress of ACC:V (1:2) paste with the volume fraction. Comparison of the experimental data with the Yodel model [22] (blue curve) and the fractal model of Shi et al.[24] (red curve).

In summary, this analysis suggests that our pastes can be considered as a dense suspension of flocs composed by aggregated colloids whose rheological properties depend of the interparticle force, particle size, surface roughness and contact area between particles. Any process modifying one of these parameters induces automatically a change of the rheological properties (elastic modulus and yield stress).

3.3.4 Discussion of final hardening of cement

The plateau value of $G' \sim 1$ MPa, reached after a few hours of aging, is very far from the shear modulus of the hardened cement of ~ 1 GPa and of a pure calcite of 35 GPa. This signifies that the elasticity of the paste is here due to weak interactions inside flocs and between branched flocs of calcite [28].

The final strength of the cement is attained with a different timescale at a later stage after the experiments presented here. We will however make some reflections on the relation to the present results. During drying the main structure is locked and does not change appreciably except for loose grains that are pulled towards the closest neighbours by capillary forces as menisci are moving during drying. Stiff grain contacts with stronger, covalent bonds are formed where weaker van der Waals forces dominated the wet paste. The elastic modulus increases by 3 orders of magnitude, probably mainly due to the shear strength of covalent forces as opposed to the lack of shear strength in wet grain contacts with vdW forces. The relatively low yield stress of ~ 1 MPa [41], however suggests that the open structure inherited from the paste results in relatively few and small covalently bounded grain contacts. This suggests that any attempt to develop calcite cements with a higher yield strength should target the recrystallization period studied here to achieve a more compact structure with larger grain contacts.

4. Conclusions

Calcium carbonate cements have been synthesized by mixing amorphous calcium carbonate and vaterite powders with water to a cement paste to study how mechanical

strength is created during the setting reaction. Two complementary tools have been used: In-situ XRD was used to monitor the phase transformation of ACC and vaterite phases into calcite and a rotational rheometer was used to monitor the strength evolution. XRD gives access to the kinetics of the phase transformations that could not be understood through rheological experiments or from previous results in fluid reactors. Viscoelastic measurements are more sensitive to interparticle forces and to the grain morphology and give access to the kinetics of grain smoothening, not detected by XRD. The combination of the two techniques allows to link microstructure to macroscopic properties.

There are two characteristic time scales of the strengthening of the cement paste. The short timescale of the order 1 hour is controlled by smoothening of the vaterite grains, allowing closer and therefore adhesive contacts between the grains. The long timescale of the order 10-50 hours is controlled by the phase transformation of vaterite into calcite. The new results of phase transformations have been analysed using a dissolution-diffusion-precipitation model that reveals that the phase transformation in a paste is limited mainly by diffusion in the liquid phase and partially by vaterite dissolution. This is contrary to previous results in fluid reactors, where calcite growth is the rate limiting.

We also found that the evolution of shear strength with solid volume fraction is best explained by a fractal model of the paste structure and that the Yodel model does not fit our data.

The final image from this study is that at short times (~1h), contact areas and attractive forces between grains increase due to grain smoothing and the phase transformation exchanges the strength bearing phase from vaterite into calcite. This exchange occurs on 10-50 hours in dense suspensions.

Acknowledgments

This project has received funding from the European Union Horizon 2020 research and innovation program under the Marie Skłodowska-Curie grant agreement no. 642976-NanoHeal Project. The results of this paper reflect only the author's view and the Commission is not responsible for any use that may be made of the information it contains. The authors would like to express gratitude to the late Ellis Gartner who suggested the preparation protocol studied here and that contributed through many discussions. J.R.-S. would like to express his thanks to Lab engineer David Wragg (University of Oslo) for his assistance analysing XRD data and to Professors Jean Colombani and Marie Le Merrer (University of Lyon) for their fruitful discussions.

References

- [1] E.M. Gartner, D.E. Macphee, A physico-chemical basis for novel cementitious binders, *Cem. Concr. Res.* 41 (2011) 736–749. doi:10.1016/j.cemconres.2011.03.006.
- [2] J.L. Provis, J.S.J. van Deventer, *Alkali Activated Materials*, Springer, 2014.
- [3] T. Zhang, C.R. Cheeseman, L.J. Vandeperre, Development of low pH cement systems forming magnesium silicate hydrate (M-S-H), *Cem. Concr. Res.* 41 (2011) 439–442. doi:10.1016/j.cemconres.2011.01.016.
- [4] H. Justnes, Alternative Low-CO₂ “Green” Clinkering Processes, *Rev. Mineral. Geochemistry.* 74 (2012) 83–99. doi:10.2138/rmg.2012.74.2.
- [5] M.-L. Fontaine, C. Combes, T. Sillam, G. Dechambre, C. Rey, New Calcium

- Carbonate-Based Cements for Bone Reconstruction, *Key Eng. Mater.* 284–286 (2005) 105–108. doi:10.4028/www.scientific.net/KEM.284-286.105.
- [6] C. Combes, B. Miao, R. Bareille, C. Rey, Preparation, physical-chemical characterisation and cytocompatibility of calcium carbonate cements., *Biomaterials*. 27 (2006) 1945–54. doi:10.1016/j.biomaterials.2005.09.026.
- [7] D. Zaelke, O. Young, S.O. Andersen, Scientific synthesis of Calera carbon sequestration and carbonaceous by-product applications. Consensus findings of the scientific synthesis team, (2011).
- [8] T. Ogino, T. Suzuki, K. Sawada, The formation and transformation mechanism of calcium carbonate in water, *Geochim. Cosmochim. Acta*. 51 (1987) 2757–2767. doi:10.1016/0016-7037(87)90155-4.
- [9] J. Wang, U. Becker, Energetics and kinetics of carbonate orientational ordering in vaterite calcium carbonate, *Am. Mineral.* 97 (2012) 1427–1436. doi:10.2138/am.2012.3990.
- [10] J.P. Andreassen, Formation mechanism and morphology in precipitation of vaterite - Nano-aggregation or crystal growth?, *J. Cryst. Growth*. 274 (2005) 256–264. doi:10.1016/j.jcrysgr.2004.09.090.
- [11] J.D. Rodriguez-Blanco, S. Shaw, L.G. Benning, The kinetics and mechanisms of amorphous calcium carbonate (ACC) crystallization to calcite, via vaterite, *Nanoscale*. 3 (2011) 265–271. doi:10.1039/c0nr00589d.
- [12] P. Bots, L.G. Benning, J.-D. Rodriguez-Blanco, T. Roncal-Herrero, S. Shaw, Mechanistic insights into the crystallization of amorphous calcium carbonate (ACC), *Cryst. Growth Des.* 12 (2012) 3806–3814. doi:10.1021/cg300676b.

- [13] F. Konrad, F. Gallien, D.E. Gerard, M. Dietzel, Transformation of Amorphous Calcium Carbonate in Air, *Cryst. Growth Des.* 16 (2016) 6310–6317. doi:10.1021/acs.cgd.6b00906.
- [14] G. Wolf, C. Günther, Thermophysical investigations of the polymorphous phases of calcium carbonate, *J. Therm. Anal. Calorim.* 65 (2001) 687–698. doi:10.1023/A:1011991124181.
- [15] M.H. Nielsen, S. Aloni, J.J. De Yoreo, In situ TEM imaging of CaCO₃ nucleation reveals coexistence of direct and indirect pathways, *Science* (80-.). 345 (2014) 1158–1162. doi:10.1126/science.1254051.
- [16] B.B. Schroeder, D.D. Harris, S.T. Smith, D.O. Lignell, Theoretical framework for multiple-polymorph particle precipitation in highly supersaturated systems, *Cryst. Growth Des.* 14 (2014) 1756–1770. doi:10.1021/cg401892b.
- [17] F.P. Carr, D.K. Frederick, Calcium carbonate, in: Kirk-Othmer (Ed.), *Kirk-Othmer Encycl. Chem. Technol.* Vol. 1 - 26, 5th Ed., John Wiley & Sons, Inc, 1967: pp. 551–556.
- [18] J.L. Banner, Application of the trace element and isotope geochemistry of strontium to studies of carbonate diagenesis, *Int. Assoc. Sedimentol.* 42 (1995) 805–824.
- [19] H. Colfen, Precipitation of carbonates: recent progress in controlled production of complex shapes, *Curr. Opin. Colloid Interface Sci.* 8 (2003) 23–31. doi:10.1016/S1359-0294.
- [20] P.O. Roehl, P.W. Choquette, *Carbonate Petroleum Reservoirs*, 1985. doi:10.1007/978-1-4612-5040-1.

- [21] R.G. Larson, *The Structure and Rheology of Complex Fluids*, Oxford Univ. Press, Oxford and New York, 1999. <http://ci.nii.ac.jp/naid/110002077498/en/>.
- [22] R.J. Flatt, P. Bowen, Yodel: A yield stress model for suspensions, *J. Am. Ceram. Soc.* 89 (2006) 1244–1256. doi:10.1111/j.1551-2916.2005.00888.x.
- [23] W.-H. Shih, W.Y. Shih, S.-I. Kim, J. Liu, I.A. Aksay, Scaling properties of mechanical properties of colloidal gel.pdf, *Phys. Rev. E.* 42 (1990) 4772–4779.
- [24] W.Y. Shih, W.-H. Shih, I.A. Aksay, Elastic and Yield Behavior of Strongly Flocculated Colloids, *J. Am. Ceram. Soc.* 82 (1999) 616–624. doi:10.1111/j.1151-2916.1999.tb01809.x.
- [25] G.H. Kirby, J.A. Lewis, Rheological Property Evolution in Concentrated Cement-Polyelectrolyte Suspensions, *J. Am. Ceram. Soc.* 85 (2004) 2989–2994. doi:10.1111/j.1151-2916.2002.tb00568.x.
- [26] R.J. Flatt, N.S. Martys, L. Bergström, *The Rheology of Cementitious Materials*, 29 (2004) 314–318.
- [27] K. Yamada, S. Ogawa, S. Hanehara, Controlling of the adsorption and dispersing force of polycarboxylate-type superplasticizer by sulfate ion concentration in aqueous phase, *Cem. Concr. Res.* 31 (2001) 375–383. doi:10.1016/S0008-8846(00)00503-2.
- [28] T. Liberto, M. Le Merrer, C. Barentin, M. Bellotto, J. Colombani, Elasticity and yielding of a calcite paste: scaling laws in a dense colloidal suspension, *Soft Matter.* 13 (2017) 2014–2023. doi:10.1039/C6SM02607A.
- [29] Weitz, D. A., *Diffusing Wave Spectroscopy*, *Dyn. Light Scatt. Method Some Appl.* (1993) 652–720.

- [30] L.N. Plummer, E. Busenberg, The solubilities of calcite, aragonite and vaterite in CO-H₂O solutions between 0 and 90°C, and an evaluation of the aqueous model for the system CaCO₃-CO₂-H₂O, *Geochimica Cosmochim. Acta.* 46 (1982) 1011–1040.
- [31] P. Cubillas, S. Köhler, M. Prieto, C. Chaïrat, E.H. Oelkers, Experimental determination of the dissolution rates of calcite, aragonite, and bivalves, *Chem. Geol.* 216 (2005) 59–77. doi:10.1016/j.chemgeo.2004.11.009.
- [32] L. Li, J.R. Sanchez, F. Kohler, A. Røyne, D.K. Dysthe, Microfluidic Control of Nucleation and Growth of CaCO₃, *Cryst. Growth Des.* 18 (2018) 4528–4535. doi:10.1021/acs.cgd.8b00508.
- [33] M.M. Reddy, L.N. Plummer, E. Busenberg, Crystal growth of calcite from calcium bicarbonate solutions at constant PCO₂ and 25°C: a test of a calcite dissolution model, *Geochim. Cosmochim. Acta.* 45 (1981) 1281–1289. doi:10.1016/0016-7037(81)90222-2.
- [34] L. Hernández, M. Gurruchaga, I. Goñi, Influence of powder particle size distribution on complex viscosity and other properties of acrylic bone cement for vertebroplasty and kyphoplasty, *J. Biomed. Mater. Res. - Part B Appl. Biomater.* 77 (2006) 98–103. doi:10.1002/jbm.b.30409.
- [35] B.E. Larsen, J. Bjørnstad, E.O. Pettersen, H.H. Tønnesen, J.E. Melvik, Rheological characterization of an injectable alginate gel system, *BMC Biotechnol.* 15 (2015) 1–12. doi:10.1186/s12896-015-0147-7.
- [36] G. Brekke-Svaland, F. Bresme, Interactions between Hydrated Calcium Carbonate Surfaces at Nanoconfinement Conditions, *J. Phys. Chem. C.* 122 (2018) 7321–

7330. doi:10.1021/acs.jpcc.8b01557.
- [37] D.F. Parsons, R.B. Walsh, V.S.J. Craig, Surface forces: Surface roughness in theory and experiment, *J. Chem. Phys.* 140 (2014). doi:10.1063/1.4871412.
- [38] J.D. Olarte-Plata, G. Brekke-Svaland, F. Bresme, Dependence of the phase behavior of suspensions of mineral nanoparticles on the particle surface roughness, *ArXiv*. (2019). <http://arxiv.org/abs/1905.07254>.
- [39] J. Dziadkowiec, S. Javadi, J.E. Bratvold, O. Nilsen, A. Røyne, Surface Forces Apparatus Measurements of Interactions between Rough and Reactive Calcite Surfaces, *Langmuir*. 34 (2018) 7248–7263. doi:10.1021/acs.langmuir.8b00797.
- [40] N. Roussel, A. Lemaître, R.J. Flatt, P. Coussot, Cement and Concrete Research Steady state flow of cement suspensions : A micromechanical state of the art, *Cem. Concr. Res.* 40 (2010) 77–84. doi:10.1016/j.cemconres.2009.08.026.
- [41] J. Rodríguez-Sánchez, Q. Zhang, D.K. Dysthe, Microstructure and relative humidity effects on long-term indentation creep properties of calcium carbonate cement, *Preprints*. (2018) 1–25. doi:10.20944/preprints201810.0671.v1.